316026

②

DEFENCE
RESEARCH
AGENCY

DTIC
S ELECTE D
MAR 1 0 1993
C

Technical Memorandum

December 1992

Heat Transfer and Aerodynamics of a 3D Design Nozzle Guide Vane Tested in the Pyestock Isentropic Light Piston Facility

by

K. S. Chana
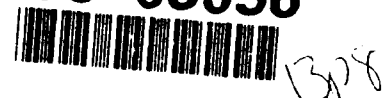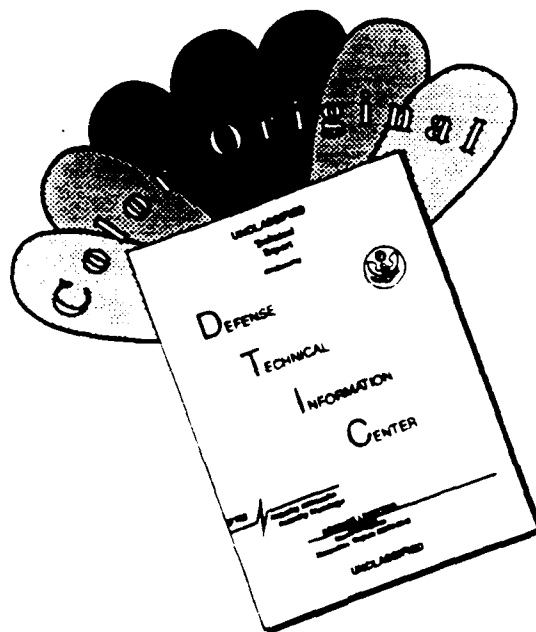
93-05056

93 3 9 012

Farnborough, Hampshire

DISCLAIMER NOTICE

THIS DOCUMENT IS BEST QUALITY AVAILABLE. THE COPY FURNISHED TO DTIC CONTAINED A SIGNIFICANT NUMBER OF COLOR PAGES WHICH DO NOT REPRODUCE LEGIBLY ON BLACK AND WHITE MICROFICHE.

DTIC QUALITY INSPECTED 2

DEFENCE RESEARCH AGENCY
Farnborough

Technical Memorandum Aerodynamic & Propulsion 19

HEAT TRANSFER AND AERODYNAMICS OF A 3D DESIGN NOZZLE GUIDE VANE TESTED IN THE PYESTOCK ISENTROPIC LIGHT PISTON FACILITY

by

K. S. Chana

SUMMARY

In HP turbines, predictions of the heat transfer to the blade and endwalls is particularly important for an accurate assessment of turbine component life. On the endwalls, there are often complex 3D (secondary) flows present which make predictions of heat transfer particularly difficult.

A detailed investigation of this area has been carried out on a fully annular cascade of highly 3D nozzle guide vanes. Measurements were made on the vane and endwalls to determine heat transfer and aerodynamic characteristics. Testing was conducted in a short duration Isentropic Light Piston test facility, at engine representative Reynolds number, Mach number and gas-to-wall temperature ratio. Interpreted test data are compared with computations obtained at test conditions.

HEAT TRANSFER AND AERODYNAMICS OF A 3D DESIGN NOZZLE GUIDE VANE TESTED IN THE PYESTOCK ISENTROPIC LIGHT PISTON FACILITY

Mr. K.S. Chana
Defence Research Agency
Aerodynamics & Propulsion Department
Pyestock, Farnborough,
Hampshire. GU14 0LS
United Kingdom.

ABSTRACT

In HP turbines, predictions of the heat transfer to the blade and endwalls is particularly important for an accurate assessment of turbine component life. On the endwalls, there are often complex 3D (secondary) flows present which make predictions of heat transfer particularly difficult.

A detailed investigation of this area has been carried out on a fully annular cascade of highly 3D nozzle guide vanes. Measurements were made on the vane and endwalls to determine heat transfer and aerodynamic characteristics. Testing was conducted in a short duration Isentropic Light Piston test facility, at engine representative Reynolds number, Mach number and gas-to-wall temperature ratio. Interpreted test data are compared with computations obtained at test conditions.

1. INTRODUCTION

In order to increase thrust-to-weight ratio and achieve maximum cycle efficiencies with gas turbine engines it is necessary to raise the cycle temperatures to the maximum, within the constraints of structural integrity. Thus the need to understand in detail and predict accurately the heat transfer distributions for high pressure turbines becomes an important factor. The presence of complex highly three-dimensional secondary flows within the turbine passage makes the turbine designer's task very difficult.

Several different investigations of nozzle guide vane (NGV) aerofoil and endwall heat transfer behaviour have been reported in the literature. The work of York et al (1983), Gladden et al, (1988) and Boyle et al (1989), concentrated on two-dimensional cascade measurements, and although general features of the flow were modelled radial pressure gradients were not. Granziani et al (1979), and Gaugler and Russell (1983), correlated detailed heat transfer measurements with secondary flow patterns. This work was not representative of engine operating conditions in terms of Reynolds number, Mach number and gas-to-wall temperature ratio. More recent work by Harasgama et al, (1990), and Harvey et al, (1990), have shown detailed information on the pattern of heat transfer within a NGV passage. However, these NGV designs incorporated relatively few three-dimensional features.

A highly three-dimensional nozzle guide vane has been designed and tested at DRA Pyestock. The prime objective was to produce a challenging three-dimensional design which would act as a stimulus for aerodynamic and thermodynamic research. Fully three-dimensional flow calculation methods were employed in the design of the variable-lean nozzle guide vane. Figure 1 shows the details of the vane and the computational grid used.

The purpose of this paper is to describe heat flux and pressure measurements obtained from a set of NGV's using the Isentropic Light Piston Facility (ILPF) a short duration heat transfer tunnel. The NGV annular ring was tested over a range of Reynolds number, Mach number and gas-to-wall temperature ratios, representative of engine conditions. The detailed measurements are compared with theoretical flow and heat transfer predictions.
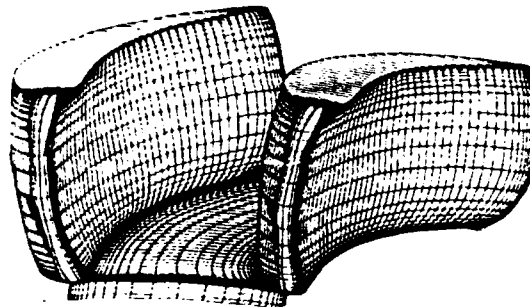

Figure 1. HTDU 4X vane and computational grid

2 DESIGN DETAILS

2.1 Duty

The aerodynamic design of the high pressure turbine was targeted for a future engine of advanced military duty. The turbine has been designated the High Temperature Demonstrator Unit (HTDU) 4X. It has the following overall design parameters.

Stator outlet temperature (SOT)	2066.1K
Specific work capacity ($Cp\Delta T/T$)	179.6 J/Kg K
Stage loading factor $\Delta H/U^2$	2.002
Stage pressure ratio	2.416
Flow function Va/U^2	0.625
NGV flow function $w\sqrt{T}/P$	1.06×10^{-3} Kg$\sqrt{K}$ m^2/$_{SN}$

converted to heat transfer rate by an electrical analogue circuit which solves the one-dimensional transient heat conduction equation (Oldfield et al, 1984). The output signal is then digitised and recorded on a mini computer. The present tests included thin film gauges at 10%, 20%, 40%, 60%, 80% and 90% spanwise locations with 12 on the suction side and 10 on the pressure side at each spanwise location. There were 82 gauges on the inner wall and 76 gauges on the outer wall. With this level of instrumentation it was possible to obtain an accurate distribution of vane surface and endwall heat transfer. Accuracy of the present heat transfer data is within ±5%. Figure 3 shows vanes instrumented with thin films.
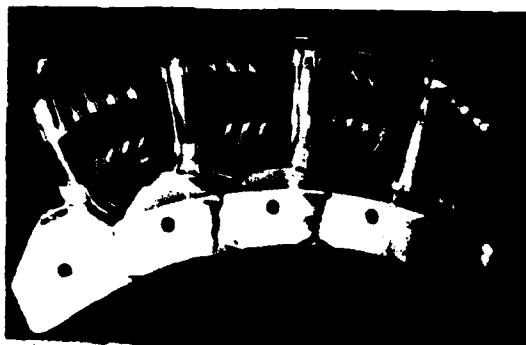

Figure 3. Vanes instrumented with thin films

The distribution of static pressure on the NGVs was measured using surface tappings, and the inlet total pressure was determined using 3 inlet probes, positioned at 120° intervals circumferentially. The pressure signals were recorded using a fast acting Scanivalve[2] ZOC (Zero, Operate, Calibrate) system. The NGVs were fitted with tappings at 5%, 10%, 20%, 40%, 60%, 80%, 90% and 95% span with 14 on the suction side and 11 on the pressure side, at each spanwise location. The inner platform was instrumented with 83 pressure tappings and the outer platform contained 77 pressure tappings. The overall accuracy for the aerodynamic results is such that the isentropic Mach numbers calculated from the measured static pressures are accurate to within ± 0.1% for transonic flow conditions. At low flow velocities the error is significantly larger, representing about 10% at 0.1 Mach number due to the smaller difference between the total and static pressures. All tests were performed with a turbulence grid at 4.5 axial chords upstream of the NGVs, giving an inlet turbulence level of 6.5%. Table 1 shows details of the NGV operating conditions.

4 AERODYNAMIC RESULTS

4.1 Surface Aerodynamics

Mach number distributions at 60% span for three Mach number conditions are shown in Figure 4. The measured Reynolds number has been kept constant for these results. The pressure side aerodynamics are

---

1 Corning Macor Trademark of Corning Macor Glass, Corning, USA

2 Scanivalve - Trademark of Scanivalve Corp, San Diego, USA

TABLE 1. TEST OPERATING CONDITIONS						
	Re.D: M.-	Re.D: M.D	Re.D: M.+	Re-: M.D	Re.D: M.D	Re+: M.D
EXIT MACH NUMBER	0.75	0.88	1.10	0.88	0.88	0.88
EXIT REYNOLDS NUMBER	2.96E6	2.96E6	2.96E6	1.48E2	2.96E6	4.44E6
GAS-TO-WALL TEMP. RATIO	1.5	1.5	1.5	1.5	1.5	1.5
INLET TURBULENCE	6.5%	6.5%	6.5%	6.5%	6.5%	6.5%

little influenced by changes in exit Mach number. The suction side results are similar for all three conditions during the initial acceleration from the leading edge to approximately 20% axial chord. The below design and design Mach number condition show diffusion once the initial acceleration peak has been reached, whereas the above design condition continues to accelerate further before diffusion takes place at approximately 85% axial chord.

Measured and predicted Mach number distributions at 60% span at the design condition are shown in Figure 5. As can be seen the Dawes code (Dawes, 1986) does not predict the suction side diffusion very well. Possible reasons for this could be inadequate modelling of the trailing edge geometry, differences between the modelled and true downstream annulus duct and the lack of grid resolution. The grid used for this prediction is 74 axial, 25 radial and 25 tangential points on a sheared H grid. The discrepancies near the leading edge on the pressure side are attributed to experimental error. The total to static pressure differences are small in this region, thus the error in isentropic Mach number becomes more significant. The remainder of the pressure surface is very well modelled.
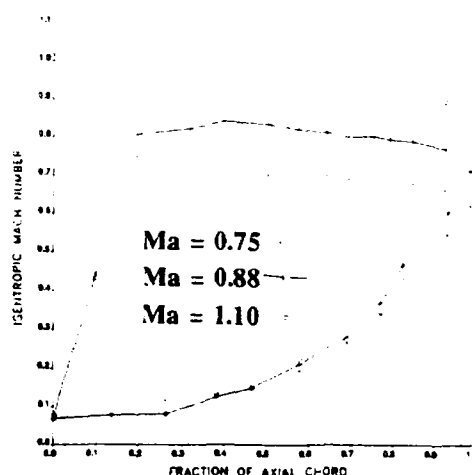

Figure 4. 60% span Mach number variation

Measured and predicted suction side isentropic Mach number distributions for three exit Mach number conditions are shown in Figure 6. Mach numbers at the vane root are higher than the tip, as required by radial equilibrium. The distributions indicate a significant change in aerodynamics as the exit Mach number is increased from the below design condition to design and above design. The predictions show similar features to the experimental results. The initial rapid acceleration is predicted well in all three cases, with some differences towards the tip.
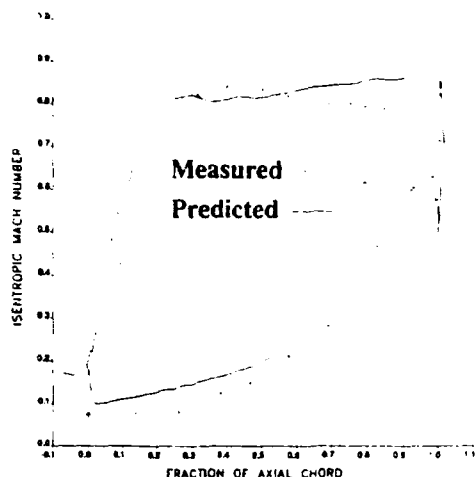
Figure 5. Vane surface Mach number distribution at 60% span.

However, this region has highly 3D geometry and is of particular difficulty for instrumenting static tappings. It is possible that some tappings may not be normal to the local surface. The vanes are manufactured by the use of a computer numerically controlled machine and are then hand finished to achieve a smooth surface particularly at the leading edge, at the junction between endwalls and the vane and at the trailing edge. This final finishing process

may have introduced small local differences in these areas.

Discrepancies towards the trailing edge of the vane vary depending on the Mach number condition. For the below design case the prediction compares very well with a few small differences near the trailing edge between 40% and 60% span. As previously discussed, the design and above design conditions show much less agreement with the prediction once the initial acceleration peak is reached. The experimental results show mainly diffusion but the prediction indicates a further acceleration.

The measured pressure side isentropic Mach number for the design condition is shown in Figure 7 together with a prediction. The prediction compares very well with the computed results. This was also true of the below and above design Mach number condition.

Hub and casing Mach number distributions for measured and predicted results are shown in Figure 8a and 8b. The hub Mach numbers exceed those on the casing due to the radial equilibrium criteria. When operating at the high Mach number condition the hub platform shows a trailing edge shock impinging on the suction surface. The comparison between measured and computed results shows very good agreement, for both hub and casing platforms. These results obviously validate the 3D Navier-Stokes code as a fast and relatively accurate method for the
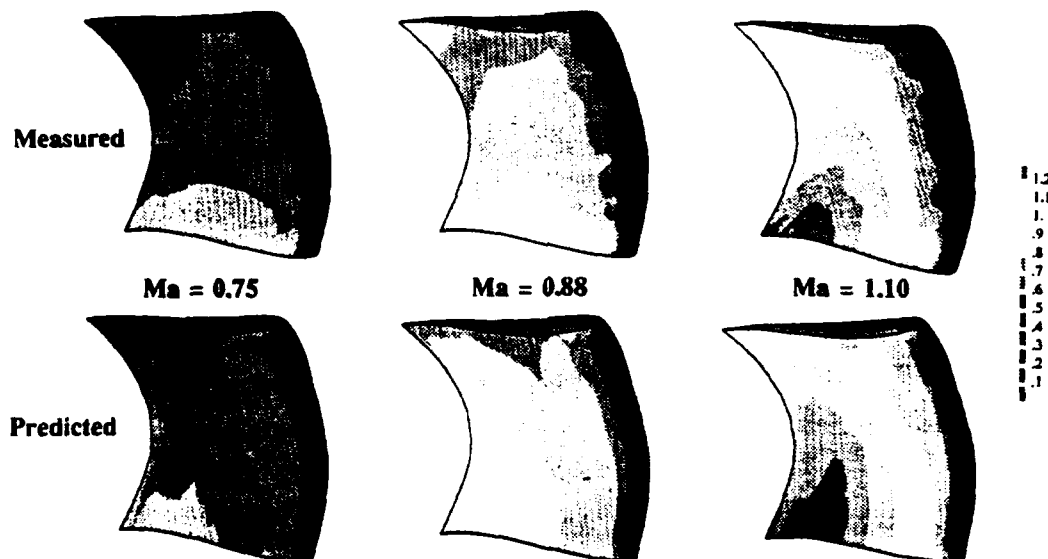

Figure 6. Comparison of measured and predicted suction surface Mach no

aerodynamic design of turbine NGVs. However, the suction side prediction towards the trailing edge could be improved further and warrants more investigation.

4.2 Exit Area Traversing

The total pressure trace obtained from the centre hole of the three hole probe together with a 3D flow (Dawes, 1986) prediction are shown in Figure 9. A small amount of digital smoothing has been applied to the measured data to remove high frequency noise. The application of 3 hole probes in the ILPF has been described by Harasgama and Chana (1990).
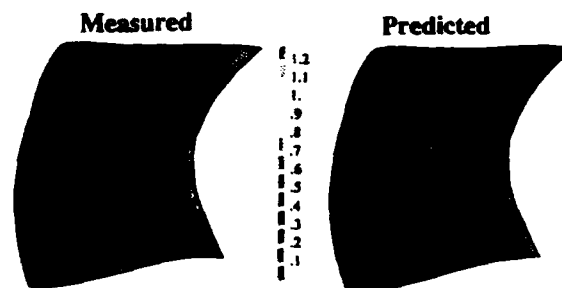

Figure 7. Comparison of measured and predicted pressure surface Mach no
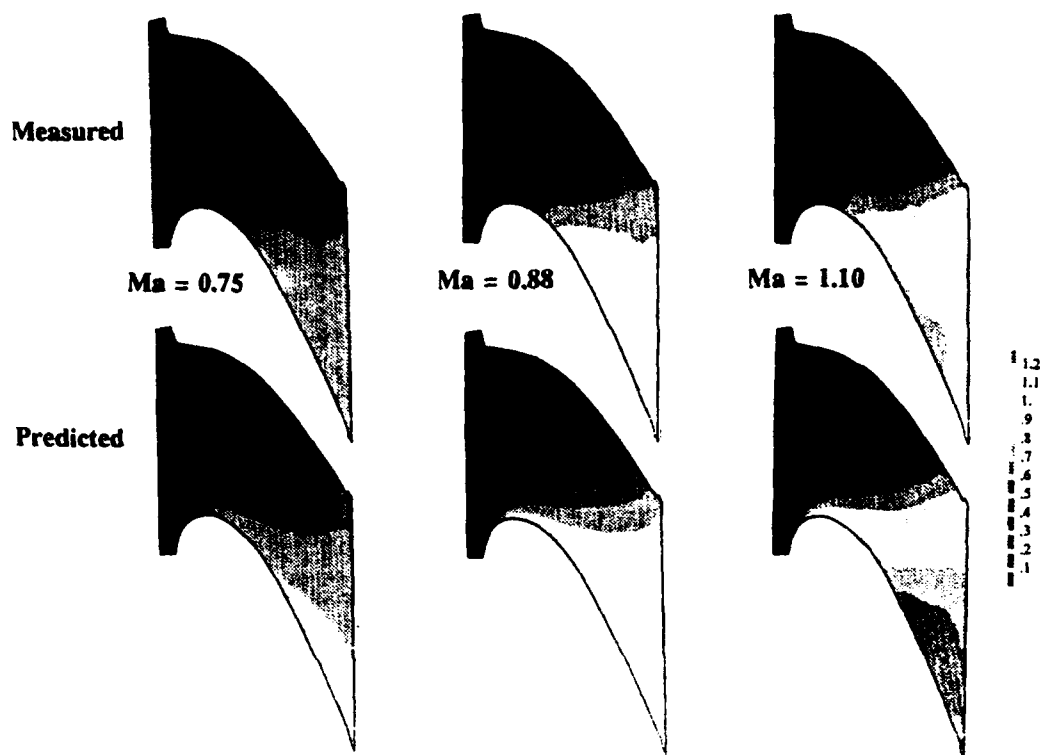
Figure 8a. Measured and predicted hub Mach number distribution

Individual experimental sweeps, after processing, have been combined to form the complete area traverse. The traverse was carried out at approximately 5% axial chord downstream of the trailing edge. The measured profile wakes can be clearly seen, at mid-height the wake is considerably wider than that near the endwalls. The wake is wider due to the trailing edge stacking; the probe tip is thus further from the trailing edge at mid-height than near the root and tip. The measured data also show areas of significant total pressure loss, these correspond to the horse-shoe vortex as seen in Figure 12a. The Navier-Stokes prediction also shows wider wakes at mid-height than near the endwalls and compares very well, although the areas of much larger loss created by the horse-shoe vortex are not predicted at all.

5   HEAT TRANSFER RESULTS

Nusselt number distributions on the vane aerofoil surface at 60% span for 5 running conditions are shown in Figure 10. As can be seen the Nusselt number increases as Reynolds number is increased, on both suction and pressure side. The variation of heat transfer with Mach number is also shown on Figure 10. In this case Nusselt number decreases with increasing Mach number. This is due to the shear stress in the boundary layer decreasing as the flow velocity increases. These results are in agreement with the work of previous authors (Jones et al, 1989).

Contours of Nusselt number overlaid onto a 3D view of the NGV suction side are presented in Figure 11. It can be seen that there is a significant effect of the secondary flow on the heat transfer distributions. The effect is seen to be more pronounced at the tip than the hub. The mid-span Nusselt numbers

towards the trailing edge are consistently higher than near the endwalls, for all operating conditions. This is due to endwall boundary layer migration onto the vane suction side resulting from secondary flow in the vane passage. Flow visualisation performed on the endwall and vane surface in the ILPC (Figure 12a and 12b) indicate that the secondary flow is stronger near the casing than at the hub. This effect is well predicted by the Dawes (1986) flow solver as can be seen in Figure 13. The hub secondary flow appears on the suction surface later than the casing and does not migrate along the span to the same extent. The prediction shows this effect but to somewhat lesser extent than indicated by the flow visualisation.

Increasing Reynolds number causes the Nusselt number over the entire vane surface to increase, whilst on the suction surface the reverse occurs for increasing Mach number. The pressure side Nusselt number distributions did not vary significantly with the Mach number changes and there is very little spanwise variation, see Figure 14.

Endwall heat transfer is affected by the inlet boundary layer, vane aerodynamic loading and the geometry of the vane passage. The tests have shown that there are some differences in the inner and outer wall Nusselt numbers both in magnitude and distribution. Figure 15 shows hub Nusselt numbers for all conditions. As the Reynolds number is increased the region of highest heat transfer becomes concentrated at the pressure side trailing edge.

The inlet endwall boundary layer stagnates at the vane leading edge and forms a horseshoe vortex. The two legs of this vortex, on the pressure and suction sides, proceed into the two adjacent passages. The pressure side leg is swept across the endwall by the
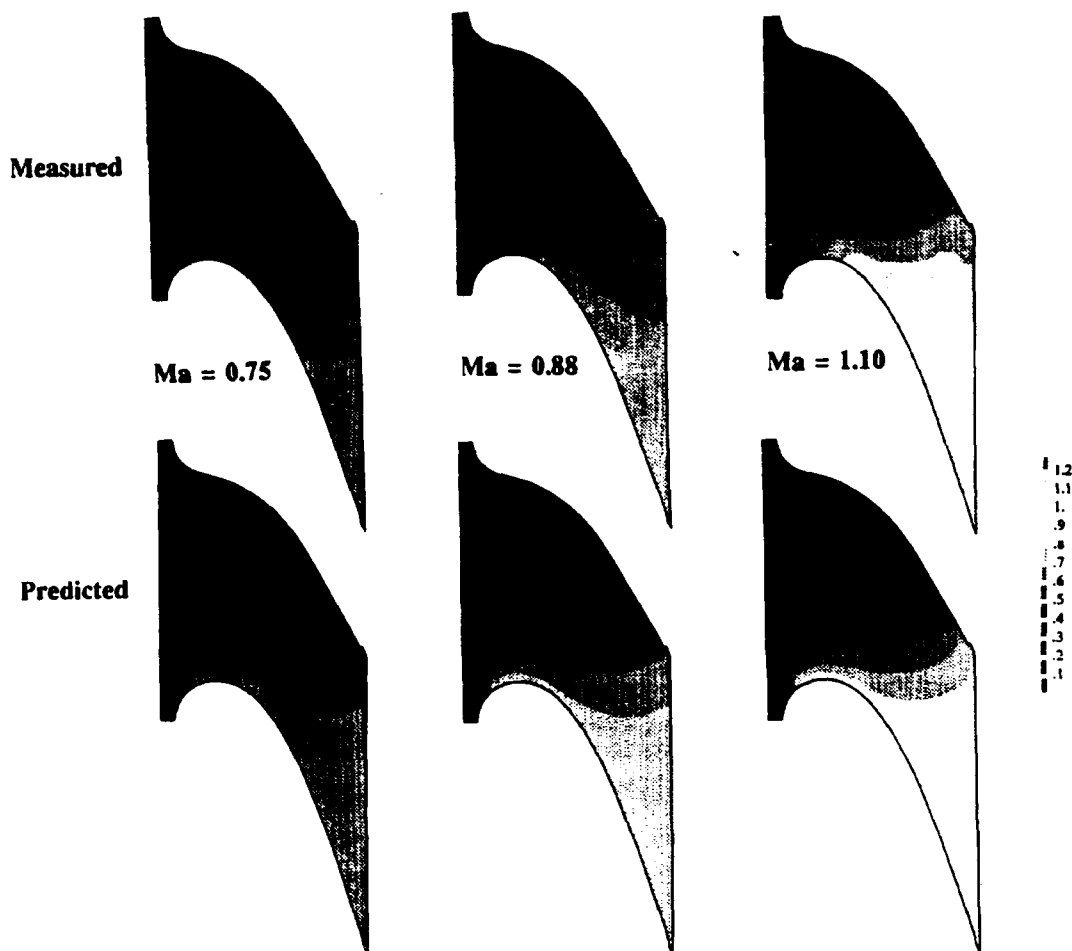
Measured

Ma = 0.75   Ma = 0.88   Ma = 1.10

Predicted

1.2
1.1
1.
.9
.8
.7
.6
.5
.4
.3
.2
.1

Figure 8b. Measured and predicted casing Mach number distribution

passage secondary vortex to the suction side and then up the vane suction surface. This causes the boundary layer to be stripped off the endwall and convected to the suction side of the passage and then up the suction surface of the vane. A new thin highly skewed boundary layer thus forms behind the

separation line, which results in high heat transfer in this region (Chana, 1992). Low values of heat transfer are evident close to the suction side of the passage after approximately 50% axial chord. This is generated by the low energy fluid migrating across from the pressure side trailing edge region. Outer
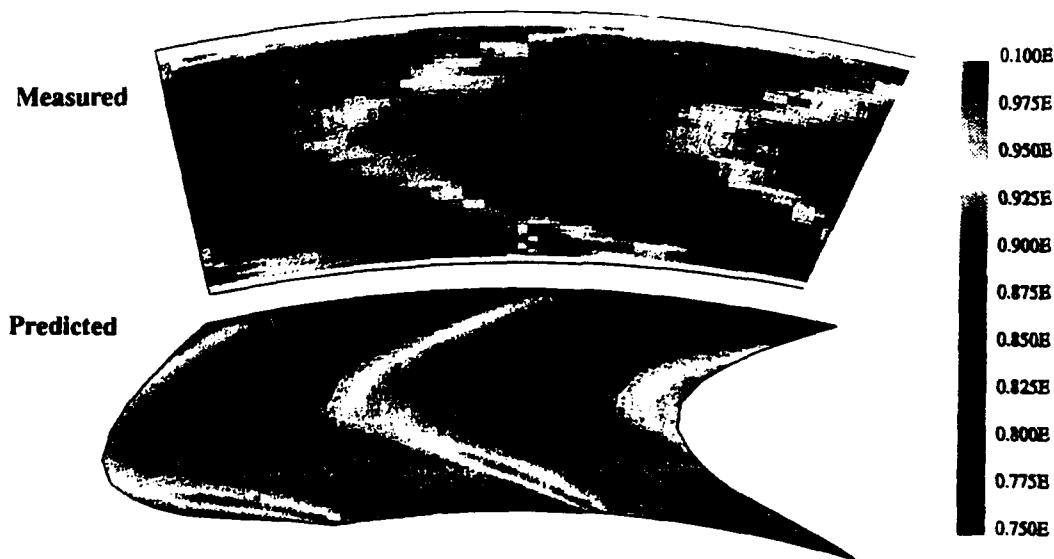

Measured

Predicted

0.100E
0.975E
0.950E
0.925E
0.900E
0.875E
0.850E
0.825E
0.800E
0.775E
0.750E

Figure 9. Measured and predicted total pressure contours 105% axial chord
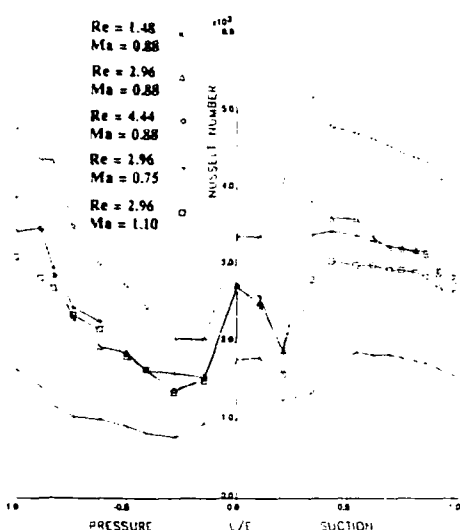
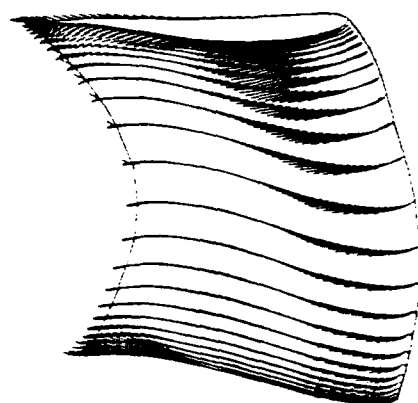Figure 10. Variation of Nusselt number for all conditions

Figure 13. Predicted flow vectors

endwall Nusselt numbers show a similar trend (Figure 16), although the distributions show lower heat transfer near the suction surface indicating a greater migration of the endwall boundary layer from the pressure side towards the suction side.
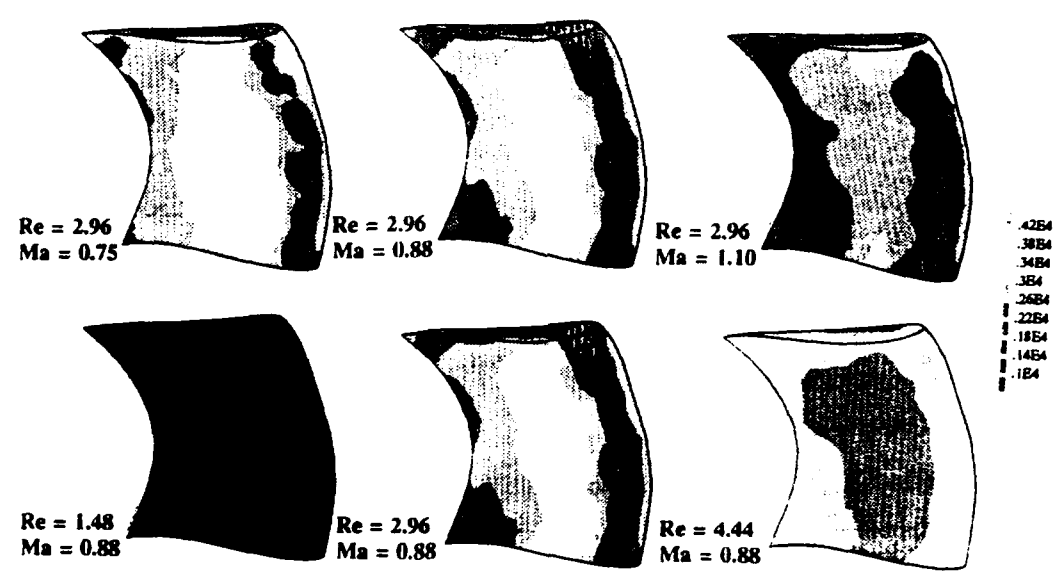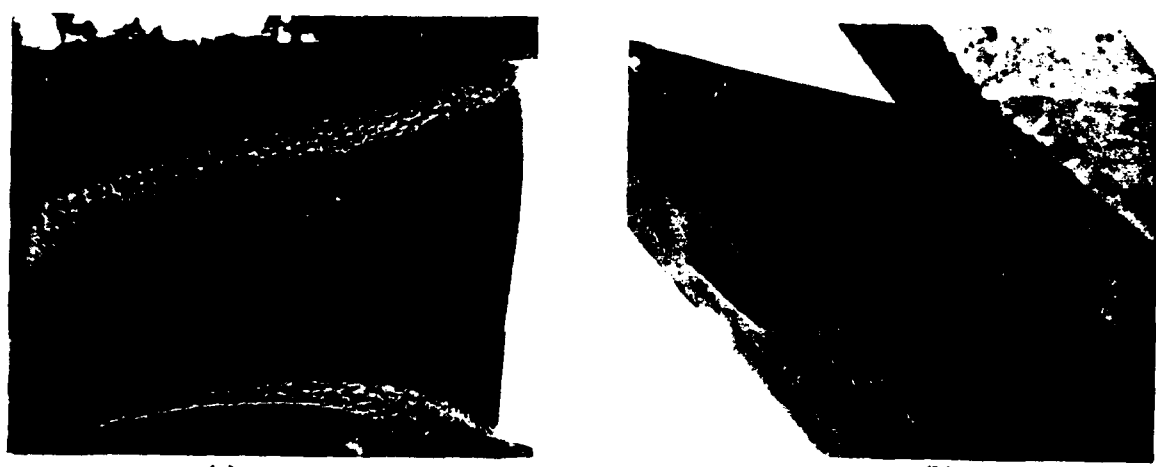

Figure 11. Suction side Nusselt number distribution

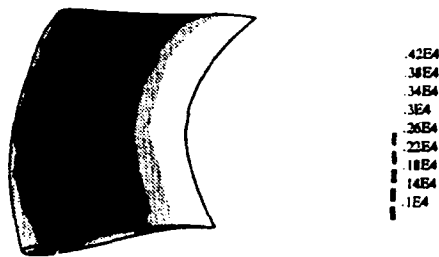(a)   Figure 12. Suction side flow visualisation   (b)

Figure 14. Pressure side Nusselt number distribution

An attempt has been made to compute the Nusselt number distribution to the vane at 60% span. Figure 17 shows measured and predicted aerofoil Nusselt numbers. The predictions were performed using versions of the Stancool and Texstan boundary layer codes (Crawford and Kays, 1976). The codes were run using the predicted pressure distribution from 3D Dawes. Two-dimensional calculations were performed along grid lines on the vane surfaces; no allowance

for surface curvature was included. The grid lines in this region follow the stream lines very closely. The inlet turbulence was set at 6.5%. The Prandtl mixing length model was used with Van Driest damping in the near wall region.

The Texstan computation was started close to the leading edge from a specified boundary layer dimension. In the case of Stancool an initial distance from the stagnation point was specified. It was found that the subsequent turbulent boundary layer development was only weakly dependent on the initial laminar region. Transition location was determined by the correlation of Abu-Ghannam and Shaw (1980) in the case of Stancool computations and a transition Reynolds number of 200 was specified for Texstan. It will be seen that transition is quite well predicted using both approaches. The heat transfer levels are in error by around 30% in the worst case, for the pressure side, but the errors are more typically 10%. The pressure surface results from Texstan show good agreement. The discrepancies towards the trailing edge are probably due to irregularities in the trailing
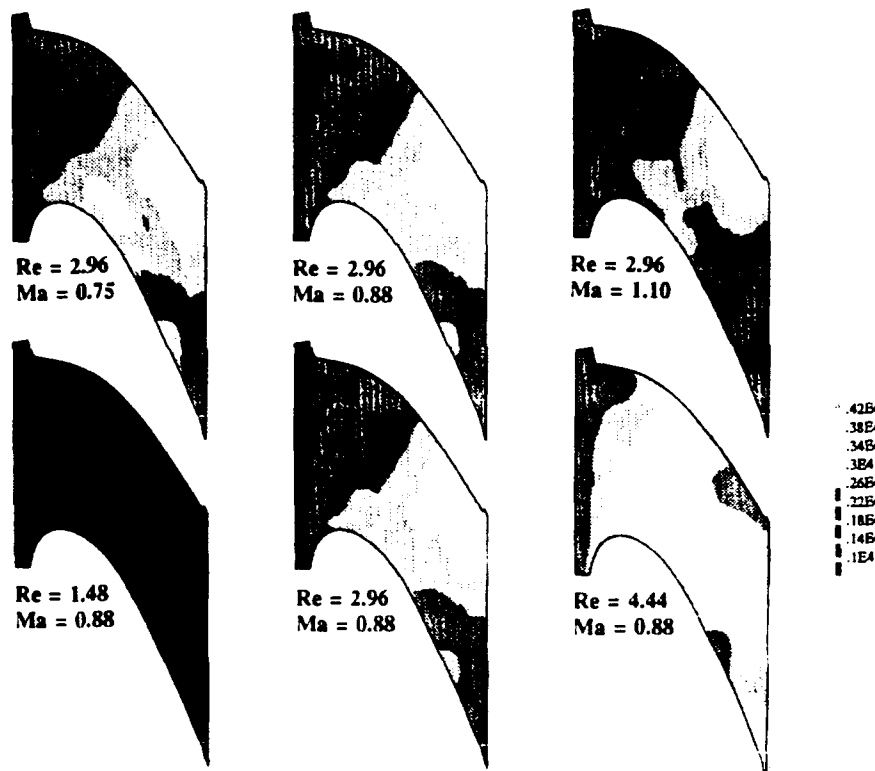

Figure 15. Hub Nusselt number distributions

edge predicted pressure distribution from Dawes, as discussed in Section 4. On the suction surface Texstan performed less well with a large over-shoot but then approached the experimental results. Stancool predicted the suction side Nusselt number distribution reasonably well but substantially under predicted on the pressure side. Stancool results with the transition location determined by a Reynolds number of 200 predicted slightly later transition and gave slightly better results.

The Texstan code used was an earlier release and did not include many of the features of the more mature Stancool code. Many refinements to the predictions

remain to be explored. These include smoothing of the imposed free stream velocity distribution, curvature specification and introduction of turbulent transport equations.

CONCLUSIONS

A highly 3-dimensional nozzle guide vane has been successfully designed and tested at engine representative conditions.

Three sets of aerodynamic measurements have been taken at different Mach number conditions. The results indicate the vane is generally operating as
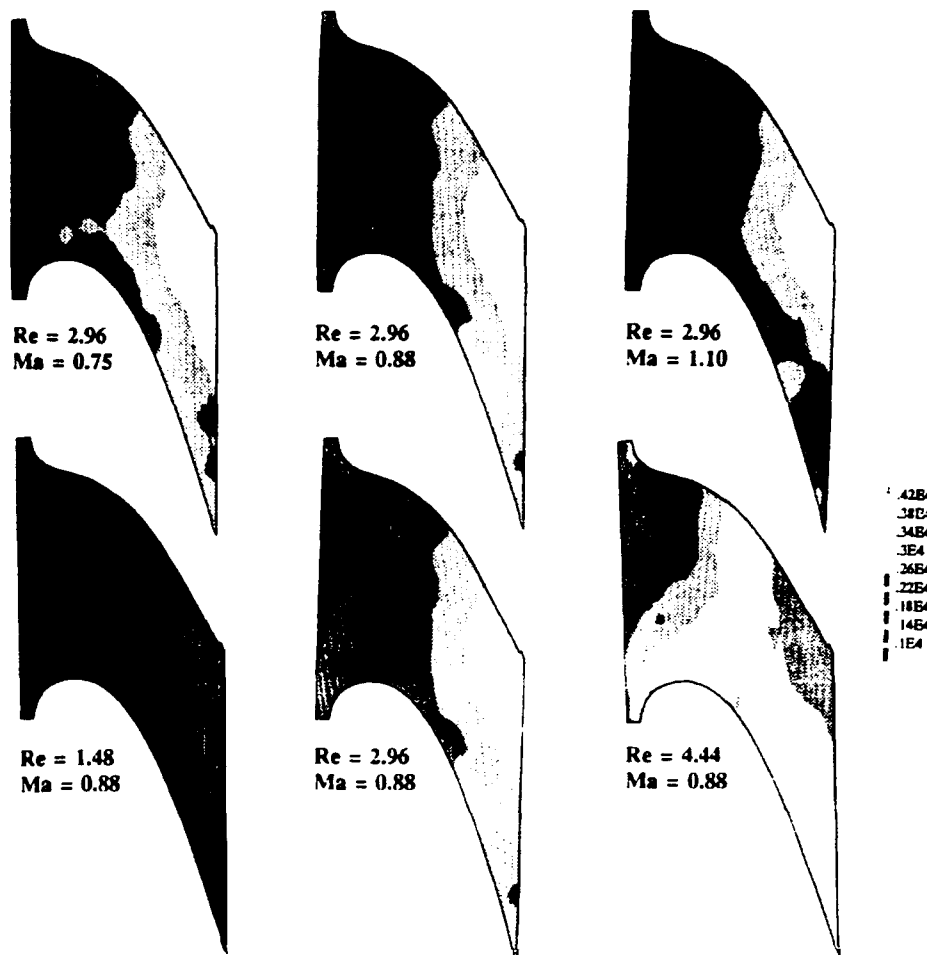
Figure 16. Casing Nusselt number distributions

designed with some unexpected behaviour towards the suction side trailing edge. This warrants further investigation. The flow visualisation of endwall cross flow indicated the presence of secondary flows and ties in with measured heat transfer patterns. Regions of high heat transfer found in other designs previously (Harasgama, 1990) in the endwall mid passage region have been reduced in area and confined to the trailing edge region. Variation of the Nusselt number with changes in Reynolds number are consistent with classical flat plate analogy. The effect of Mach number variation on Nusselt number confirms results reported by other authors.

All the measurements and predictions indicate that the secondary flows present are strongest near the casing. The downstream area traversing technique has produced good results, and these compare well with those predicted using the 3D Dawes Navier Stokes solver. However the computations made so far show no evidence of the endwall horse-shoe vortices.

Boundary layer heat transfer calculations at 60% span on the vane surfaces are promising. Transition was well predicted using either a Reynolds number of 200 or the correlation of Abu-Ghannam and Shaw. Predicted heat transfer levels are in error by typically 10% with a worse case error of 30%. Further work is obviously required to resolve inconsistencies and refine the results.

Figure 17. Predicted and measured aerofoil Nusselt number at 60% span

ACKNOWLEDGEMENTS

10

NOMENCLATURE

Cp	-	Specific heat at constant pressure
ΔH	-	Enthalpy change
Mn	-	Isentropic Mach number
Re	-	Reynolds number based on true chord
P	-	Total pressure
T	-	Total temperature
ΔT	-	Temperature change
Va	-	Axial Velocity
U	-	Mean Blade Speed

REFERENCES

Gaugler, R.E.
Russell, L.M.
'Comparison of visualised turbine endwall secondary flows and measured heat transfer patterns" NASA Technical memorandum - TM 83016, 1983

York, R.E.
Hylton, L.D.
Mihelc, M.S.
"An experimental investigation of endwall heat transfer and aerodynamics in a linear vane cascade" ASME Paper 83-GT-52, 1983

Horton, G.C.
Harasgama, S.P.
Chana, K.S.
"Predictions and measurements of three-dimensional viscous flow in a transonic turbine nozzle guide vane" AGARD CPP Paper 19, 1991

Harasgama, S.P.
Chana, K.S.
"Turbine nozzle guide vane exit area traversing in a short duration light piston test facility' 10th International Symposium Measuring Techniques for transonic and supersonic flows in cascades and turbomachines, 1990

Granziani, R.A.
Blair, M.F.
Taylor, J.R.
Mayle, R.E.
"An experimental study of endwall and airfoil surface heat transfer in a large scale turbine blade cascade" ASME Paper 79-GT-99

York, R.E
Hylton, L.D.
Mihelc, M.S.
Turner, E.R.
"Experimental investigations of turbine endwall heat transfer" Final reports I-III. Aero Propulsion Labs, Wright Patterson Air Force Base, AFWAL TR-81-2077, 1981

Schultz, D.L.
Jones, T.V.
"Heat transfer measurements in short duration hypersonic facilities' AGARD-AG-165, 1973

Dawes, W.N.
"A numerical method for the analysis of three-dimensional viscous compressible flow in a turbine cascade: application to secondary flow development in a cascade with and without dihedral' ASME Paper 86-GT-145, 1986

Crawford, M.E.
Kays, W.M.
"STAN5 a program for numerical computation of two dimensional internal and external boundary layers" NASA-CR 2742, 1976

Oldfield, M.L.G.
Burd, H.J.
Doe, N.C.
"Design of wide bandwidth analogue circuits for heat transfer instrumentation in a transient tunnel" 16th Symposium of ICHMT, Hemisphere Publication, Dubrovnik, 1984

Brooks, A.J.
Colbourne, D.E.
Wedlake, E.T.
Jones, T.V.
Oldfield, M.L.G.
Schultz, D.L.
Loftus, P.J.
'The isentropic light piston cascade at RAE Pyestock" AGARD-CP-390, 1985

Gladden, H.J.
Simoneau, R.J.
"Review and assessment of the database and numerical modelling for turbine heat transfer" 33rd ASME International Gas Turbine Congress, 1988

Harasgama, S.P.
Wedlake, E.T
"Heat transfer and aerodynamics of a high rim speed turbine nozzle guide vane treated in the RAE isentropic light piston cascade (ILPC)" ASME Paper 90-GT-41

Chana, K.S.
'Heat transfer and aerodynamics of a high rim speed turbine nozzle guide vane with profiled endwalls" ASME Paper 92-GT-243

Harvey, N.W.
Jones, T.V.
"Measured and calculation of endwall heat transfer and aerodynamics on a nozzle guide vane in annular cascade" ASME Paper 90-GT-301

Jones, T.V.
Harvey, N.W
Ireland, P.T.
Wang, Z.
"Detailed heat transfer measurements in nozzle guide vane passages in linear and annular cascades in the presence of secondary flows' AGARD Luxembourg, 1989

Abu-Ghannam, B.J.
Shaw, R.
"Natural transition of boundary layers. The effects of turbulence, pressure, and flow history". J Mech Engr. Science Vol 22, No 5, 1980.

0142412   316026

....   DRIC U

....   DRIC Y

Reports quoted are not necessarily available to members of the public or to commercial
organisations.

REPORT DOCUMENTATION PAGE

Overall security classification of this page

1. DRIC Reference (to be added by DRIC)	2. Originator's Reference DRA TM AERO/PROP 19	3. Agency Reference	4. Report Security Classification/Marking UNLIMITED

5. DRIC Code for Originator 7674300E	6. Originator (Corporate Author) Name and Location DRA Pyestock, Farnborough, Hampshire, GU14 0LS
5a. Sponsoring Agency's Code	6a. Sponsoring Agency (Contract Authority) Name and Location

7. Title

Heat Transfer and Aerodynamics of a 3D Design Nozzle Guide Vane Tested in the Pyestock Isentropic Light Piston Facility

7a. (For Translations) Title in Foreign Language

7b. (For Conference Papers) Title, Place and Date of Conference

AGARD 80th Symposium of the Propulsion and Energetics Panel on Heat Transfer and Cooling in Gas Turbines, 12-16 October 1992, Antalaya, Turkey.

8. Author 1, Surname, Initials Chana, K.S.	9a. Author 2	9b. Authors 3,4 ...	10. Date December 1992	Pages 12	Refs 17
11. Contract Number	12. Period	13. Project	14. Other Reference Nos.		

15. Distribution statement

(a) Controlled by – Unlimited distribution

(b) Special limitations (if any) –

If it is intended that a copy of this document shall be released overseas refer to DRA Leaflet No. 3 to Supplement 6 of MOD Manual 4

16. Descriptors (Keywords)   (Descriptors marked * are selected from TEST)

17. Abstract

In HP turbines, predictions of the heat transfer to the blade and endwalls is particularly important for an accurate assessment of turbine component life. On the endwalls, there are often complex 3D (secondary) flows present which make predictions of heat transfer particularly difficult.

A detailed investigation of this area has been carried out on a fully annular cascade of highly 3D nozzle guide vanes. Measurements were made on the vane and endwalls to determine heat transfer and aerodynamic characteristics. Testing was conducted in a short duration Isentropic Light Piston test facility, at engine representative Reynolds number, Mach number and gas-to-wall temperature ratio. Interpreted test data are compared with computations obtained at test conditions.

F5910/1

DRA Form A143 (revised January 1992)